

■ ORIGINAL LABORATORY RESEARCH REPORT

OPEN

Spinal Cord Stimulation Alleviates Neuropathic Pain by Attenuating Microglial Activation via Reducing Colony-Stimulating Factor 1 Levels in the Spinal Cord in a Rat Model of Chronic Constriction Injury

Cong Sun, MD,*† Xueshu Tao, MD,* Chengfu Wan, MD,* Xiaojiao Zhang, MS,* Mengnan Zhao, MD,* Miao Xu, MS,* Pinying Wang, MD,* Yan Liu, MD,* Chenglong Wang, MD,* Qi Xi, MD,* and Tao Song, MD, PhD*

BACKGROUND: Spinal cord stimulation (SCS) is an emerging, minimally invasive procedure used to treat patients with intractable chronic pain conditions. Although several signaling pathways have been proposed to account for SCS-mediated pain relief, the precise mechanisms remain poorly understood. Recent evidence reveals that injured sensory neuron-derived colony-stimulating factor 1 (CSF1) induces microglial activation in the spinal cord, contributing to the development of neuropathic pain (NP). Here, we tested the hypothesis that SCS relieves pain in a rat model of chronic constriction injury (CCI) by attenuating microglial activation via blocking CSF1 to the spinal cord.

METHODS: Sprague-Dawley rats underwent sciatic nerve ligation to induce CCI and were implanted with an epidural SCS lead. SCS was delivered 6 hours per day for 5 days. Some rats received a once-daily intrathecal injection of CSF1 for 3 days during SCS.

RESULTS: Compared with naive rats, CCI rats had a marked decrease in the mechanical withdrawal threshold of the paw, along with increased microglial activation and augmented CSF1 levels in the spinal dorsal horn and dorsal root ganglion, as measured by immunofluorescence or Western blotting. SCS significantly increased the mechanical withdrawal threshold and attenuated microglial activation in the spinal dorsal horn in CCI rats, which were associated with reductions in CSF1 levels in the spinal dorsal horn and dorsal roots but not dorsal root ganglion. Moreover, intrathecal injection of CSF1 completely abolished SCS-induced changes in the mechanical withdrawal threshold and activation of microglia in the spinal dorsal horn in CCI rats.

CONCLUSIONS: SCS reduces microglial activation in the spinal cord and alleviates chronic NP, at least in part by inhibiting the release of CSF1 from the dorsal root ganglion ipsilateral to nerve injury. (*Anesth Analg* 2022;135:178–90)

KEY POINTS

- **Question:** Is alteration of colony-stimulating factor 1 (CSF1) in the spinal cord a mechanism accounting for spinal cord stimulation (SCS)-induced analgesia?
- **Findings:** SCS might relieve neuropathic pain (NP) through microglial deactivation by inhibiting the release of CSF1 from the dorsal root ganglion to the spinal cord.
- **Meaning:** This study provides new insight into the mechanisms by which SCS alleviates chronic NP

GLOSSARY

ANOVA = analysis of variance; **ATP** = adenosine triphosphate; **BCA** = bicinechonic acid; **CCI** = chronic constriction injury; **CD11b** = integrin subunit alpha M; **CNS** = central nervous system; **CSF1** = colony-stimulating factor 1; **DH** = spinal dorsal horn; **DR** = dorsal root fiber; **DRG** = dorsal root ganglion; **GABA** = gammaaminobutyric acid; **GAPDH** = glyceraldehyde-3-phosphate dehydrogenase; **GCT** = gate control theory; **IF** = immunofluorescence; **IL** = interleukin; **ITGAM** = integrin subunit alpha M; **MoT** = motor threshold; **mRNA** = messenger ribonucleic acid; **NP** = neuropathic pain; **OCT** = optimal cutting temperature; **PCR** = polymerase chain reaction; **PFA** = paraformaldehyde; **PVDF** = polyvinylidene fluoride; **PWT** = paw withdrawal threshold; **RNA** = ribonucleic acid; **rTMS** = repetitive transcranial magnetic stimulation; **SCS** = spinal cord stimulation; **SEM** = standard error of the mean; **TBS-T** = tris-buffered saline with Tween 20; **TNF- α** = tumor necrosis factor- α

Spinal cord stimulation (SCS) for pain control is based on the concept of gate control theory (GCT) proposed by Melzack and Wall¹ in 1965. SCS-induced pain relief can last for a period of time even after the termination of stimulation, which cannot be explained by the gating theory. Previous studies have suggested that SCS alleviates pain by activating axons to produce numbness that masks the pain or by activating intermediate neurons in the spinal horn to induce brain chemical release, including serotonin, epinephrine, gamma aminobutyric acid (GABA), acetylcholine, and adenosine.^{2,3} However, the precise mechanisms underlying pain relief by SCS remain poorly understood.

Glial cells consisting of microglia, astrocytes, and oligodendrocyte lineage cells make up a significant portion of the central nervous system (CNS)^{4,5} and are now considered to play an important role in the development and maintenance of neuropathic pain (NP).^{6,7} An *in vitro* study showed that electrical stimulation of astrocytes induced an increase in the intracellular calcium concentration, which promoted glutamate release.⁸ Other research showed that repetitive transcranial magnetic stimulation (rTMS) (25 Hz) for 8 weeks reduced the activation of microglia and astrocytes by 30% in a rat model of spinal cord injury.⁹ Microglia constitute <20% of spinal glial cells under healthy conditions; however, they grow and spread quickly in the CNS after nerve injury.^{6,10–12} It has been demonstrated that microglia in the spinal cord can be activated by colony stimulating factor 1 (CSF1) derived from nerve-injured dorsal root ganglion (DRG) neurons.¹³ Activated microglial cells release cytokines, chemokines, such as interleukin (IL)-1 β , tumor necrosis factor (TNF)- α , and free radicals that are closely related to the development of NP.^{12,14} In animals with nerve injury, conventional SCS (60 Hz, 75%–90% motor threshold [MoT], and 6 hours) could produce effective analgesia and attenuate microglial

activation in the spinal dorsal horn (DH).¹⁵ MoT represents the minimum stimulus intensity that can induce muscle contraction in the trunk or hind limbs of the rats. Shinoda et al¹⁶ suggested that SCS can treat NP by inhibiting microglial activation in a rat model of spared nerve injury. However, the critical pathway leading to the reduced activity of microglia by SCS is unclear. In the present study, we examined whether SCS relieves chronic NP by attenuating microglial activation via inhibiting CSF1 to the spinal cord in a rat model of chronic constriction injury (CCI).

METHODS

Animals

Sprague-Dawley rats (males weighing 280–320 g) were purchased from SPF Biotechnology. The rats were housed under a 12/12-hour light/dark cycle with free access to water and food. The animal experiments were performed according to the Guiding Principles for Research Involving Animal and Human Beings, and the experimental procedures were approved by the Animal Care and Use Committee of China Medical University (IACUC No. 202002001).

Production of CCI Model

The CCI rat model was produced based on previous studies with minor modification.^{17–19} Briefly, rats were anesthetized with 1% to 2% isoflurane, and a 1- to 1.5-cm incision was made about 0.5 cm below the right posterior superior iliac spine. The muscle was bluntly separated to expose the sciatic nerve. The sciatic nerve was separated and ligated with 5–0 silk suture at an interval of 1 mm, with a total of 4 ligations, to just occlude but not arrest epineurial blood flow.

Implantation of the Electrode

On day 7 after CCI, rats were implanted with a custom-made electrode (0.75 mm in diameter with 4-contact electrodes). Briefly, rats were anesthetized with 2% isoflurane, the T13 lamina was exposed, and a microchannel was created using a miniature handheld craniocerebral drill (78001, RWD). The electrode was implanted into the epidural space and was carefully moved to the level of the T10–12 vertebra, corresponding to the T13–L1 spinal segment. To verify the position of the electrodes, X-rays were taken using the MultiFocus Digital Radiography Imaging System (Faxitron Bioptics LLC). Starting from day 13 after CCI, SCS (frequency, 60 Hz; pulse width, 240 μ s; intensity, 80% MoT; duration, 6 hours) was performed under 1% to 2% isoflurane anesthesia for 5 consecutive days (Figure 1). It has been suggested in this study that 80% MoT represents the maximum intensity of SCS that can be applied without causing discomfort in awake animals.¹⁹

From the *Department of Pain Medicine, First Affiliated Hospital, China Medical University, Shenyang, China; and †Department of Pain Medicine, People's Hospital affiliated to China Medical University, Shenyang, China.

Accepted for publication February 15, 2022.

Funding: None.

The authors declare no conflicts of interest.

Supplemental digital content is available for this article. Direct URL citations appear in the printed text and are provided in the HTML and PDF versions of this article on the journal's website (www.anesthesia-analgesia.org).

Address correspondence to Tao Song, MD, PhD, Department of Pain Medicine, First Affiliated Hospital, China Medical University, No. 155 Nanjing N St, Shenyang 110001, China. Address e-mail to songtaocmu@163.com.

Copyright © 2022 The Author(s). Published by Wolters Kluwer Health, Inc. on behalf of the International Anesthesia Research Society.

This is an open-access article distributed under the terms of the Creative Commons Attribution-Non Commercial-No Derivatives License 4.0 (CCBY-NC-ND), where it is permissible to download and share the work provided it is properly cited. The work cannot be changed in any way or used commercially without permission from the journal.

DOI: 10.1213/ANE.0000000000006016

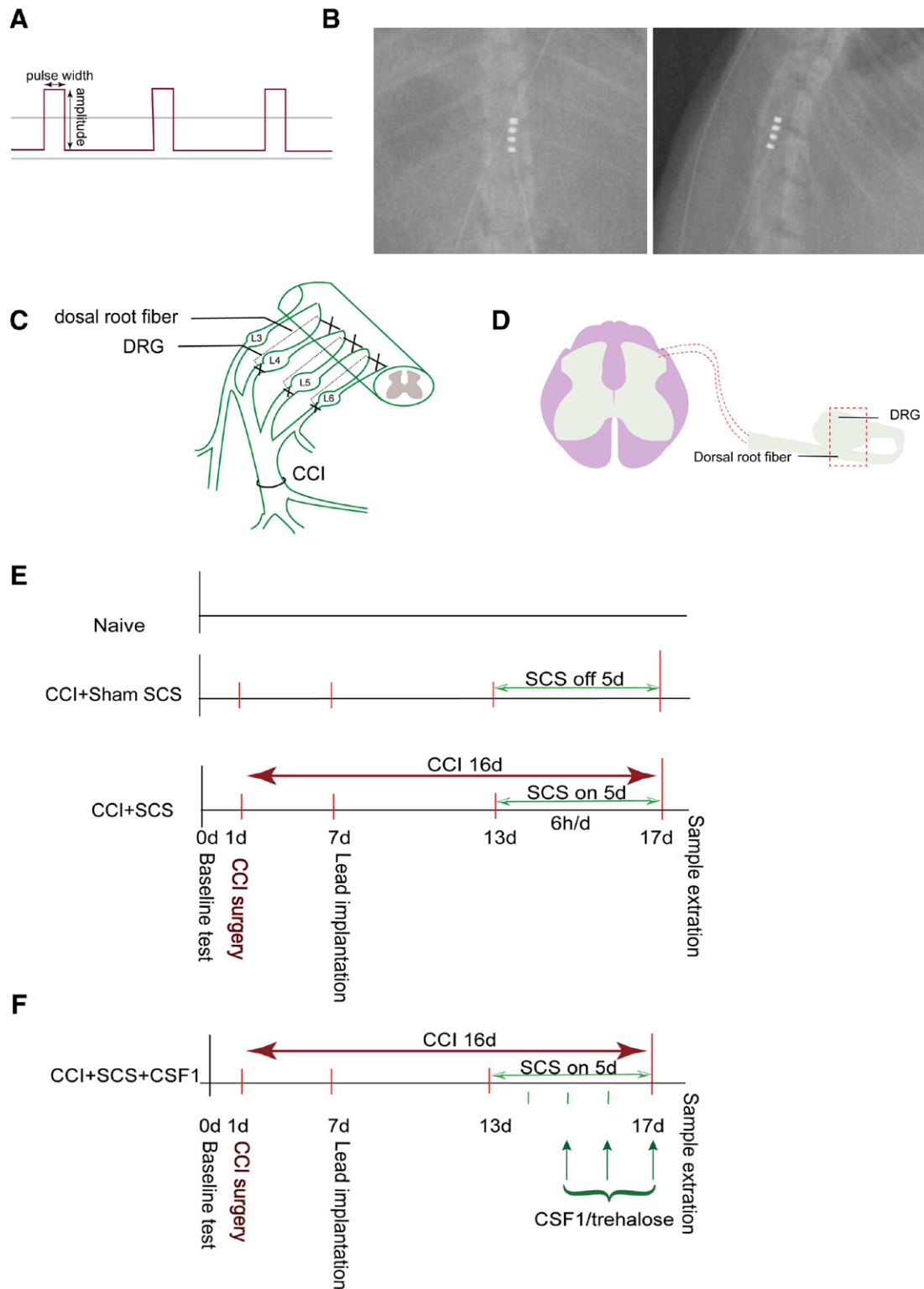


Figure 1. Stimulation mode and the experimental timeline. A, Stimulation mode: frequency, 60 Hz; pulse width, 240 μ s; intensity, 80% MoT; duration, 6 h, for 5 consecutive days. B, Representative X-ray images showing epidural placement of the SCS lead. C, Pattern diagram of extracting the DRG and DR. D, Pattern diagram of the immunofluorescence image area of a DRG with the DR. E, Experimental timeline showing CCI, electrode implantation, and SCS. F, Experimental timeline showing CCI, electrode implantation, SCS, and intrathecal injection of CSF1 or trehalose. CCI indicates chronic constriction injury; CSF1, colony-stimulating factor 1; DR, dorsal root fiber; DRG, dorsal root ganglion; MoT, motor threshold; SCS, spinal cord stimulation.

Intrathecal Injections

On day 2 after SCS, a once-daily intrathecal injection of CSF1 or trehalose was performed for 3 days in CCI + SCS rats, starting 30 minutes before SCS (Figure 1). The procedure of intrathecal injection and the dosage of CSF1 and trehalose were based on previous studies.¹³ CSF1 or trehalose was delivered in a volume of 10 μL at a concentration of 15 $\text{ng } \mu\text{L}^{-1}$ or 1 $\mu\text{mol } \mu\text{L}^{-1}$, respectively.

Behavioral Test

Mechanical hypersensitivity was tested by measuring the paw withdrawal thresholds (PWTs) in response to stimulation of von Frey filaments, as described previously.^{20–22} PWT was assessed using a dynamic plantar esthesiometer (Ugo Basile). The maximum force was limited to 50 g to avoid paw injury. The withdrawal response was automatically recorded by the aesthesiometer. Each animal was tested 3 times with a separation of 5 minutes between tests, and the mean value of the PWT was calculated. Animals were tested once every other day before surgery to determine the baseline threshold. Behavioral testing took place depending on the protocol. For the behavioral tests, the investigator was blinded to the groups.

Western Blotting Analysis

The spinal cord (L4–L6 segments) was dissected and homogenized in ice-cold lysis buffer (P0013, Beyotime) containing protease inhibitor cocktail (R0010, Solarbio). Tissue lysates were centrifuged at $12,000 \times g$ for 15 minutes at 4 °C, and the supernatants were collected for subsequent analysis. The protein concentration was determined using a bicinchoninic acid (BCA) protein assay kit (Beyotime). Protein samples (30–50 μg per lane) were separated using 8% sodium dodecyl sulfate-polyacrylamide gel electrophoresis and transferred to a polyvinylidene fluoride (PVDF) membrane (IPVH00010; Millipore). Membranes were blocked for 1 hour in Tris-buffered saline containing 0.1% Tween-20 (TBS-T), followed by overnight incubation at 4°C with the primary mouse antibodies against CSF1 (Santa Cruz Biotechnology) and glyceraldehyde-3-phosphate dehydrogenase (GAPDH; Proteintech). After washing with TBS-T, the membranes were incubated with secondary antimouse antibody (Invitrogen) for 1 hour. Immunoreactive proteins were visualized with enhanced chemiluminescence (Biosharp), and images were acquired using a luminescent image analyzer (a ChemiDoc MP Imaging System, Bio-Rad). All images were analyzed by Image J (NIH). The results were normalized to GAPDH.

Immunofluorescence

Rats were killed using an overdose of isoflurane and perfused transcardially with 4% paraformaldehyde

(PFA). Spinal cord tissue (L4–L6 segments), DRG (L4–L6 segments), and the dorsal roots (L4–L6 segments) from the spinal cord to the DRG (Figure 1), as reported by Agrawal and Evans,²³ were quickly removed. These tissues were fixed overnight in 4% PFA at 4 °C, cryoprotected with 30% sucrose for 2 days, and then frozen on dry ice with Tissue-Tek optimal cutting temperature (OCT) (Compound 4583, Sakura Finetek USA, Inc). The spinal cords were cut into 30- μm slices using a frozen microtome and floated in PBS. The DRG and dorsal roots were sliced into 14- μm longitudinal sections. For double staining of the spinal cords, sections were incubated with primary antibodies against CSF1 (1:250, Invitrogen) and CD11b (also known as integrin subunit alpha M [ITGAM]) (1:400, BIO-RAD, MCA275R) overnight at 4 °C. On the second day, the sections were incubated with the following secondary antibodies: Alexa Fluor 488 Goat antiRabbit (1:400, ThermoFisher; A11001) and Alexa Fluor 594 Goat antimouse (1:400, ThermoFisher; A11037). The DRG and dorsal root sections were incubated with primary antibodies against CSF1 (1:250, Invitrogen; PA5-42558) overnight at 4 °C. On the second day, the sections were incubated with Alexa Fluor 594 Goat antimouse secondary antibody (1:400, ThermoFisher; A11037). All images were captured using a confocal laser scanning microscope (Leica TC [Leica]) or Nikon C2 (Nikon).

Quantitative Real-Time Reverse Transcription Polymerase Chain Reaction

Total ribonucleic acid (RNA) from the spinal cord was isolated using TRIzol reagent (Invitrogen). RNA was reverse transcribed with a reverse transcription kit (Takara). Quantitative polymerase chain reaction (PCR) was performed using Power SYBR Green PCR Master Mix (Applied Biosystems) on an Applied Biosystems 7300 Real Time PCR System. All messenger RNA (mRNA) data were corrected by GAPDH and expressed as fold changes relative to the naive group. The sequences for each primer pair were as follows:

IL-6 (encoding interleukin 6): ACTTCCAGCCAGTT
G C C T T C T T G / T G G T C T G T T G T G G G
TGGTATCCTC;
IL-1 β (encoding interleukin 1 beta): CTCACAGCAGC
ATCTCGACAAGAG / TCCACGGGCAAG
ACATAGGTAGC;
TNF- α (encoding tumor necrosis factor alpha): ATGGG
C T C C C T C T C A T C A G T T C C / G C T C C T
CCGCTTGGTGGTTTG;
CD11b: GTGCTGGGAGATGTGAATGGAGAC/
GGTACTGATGCTGGCTACTGATGC;
GAPDH: GTCGGTGTGAACGGATTTG/TCCCATT
CTCAGCCTTGAC.

Statistical Analysis

Data are expressed as the means \pm standard errors of the mean (SEMs).

Statistical analyses were performed using GraphPad Prism 8.0. The results of the biochemical data were analyzed using the Student *t* test when comparing 2 groups, or 1-way analysis of variance (ANOVA) followed by Dunnett's multiple comparisons when comparing >2 groups. The results of the PWT data were analyzed using a 2-way ANOVA with repeated measurements and post hoc multiple-comparison Bonferroni tests. $P < .05$ was considered statistically significantly.

The sample size in the early stage of the experiment was mainly based on the sample size reported in the previously published studies.^{15,24} Additionally, the sample size was also calculated through experimental design and conventional numerical settings using G Power (the effect size of 0.3, a type 1 error [$P = .05$], and 80% power). For example, in the behavioral experiment to assess the mechanical hyperalgesia between naive rats and CCI rats (2-way repeated-measures ANOVA), supposed sample size calculated by G Power was 9 animals per group; we used 10 animals per group in our study. The number of animals used for each experiment and the time points for tissue collection are presented in Supplemental Digital Content, Table 1, <http://links.lww.com/AA/D914>.

RESULTS

CCI Induces Mechanical Hyperalgesia, Upregulation of CSF1, and Activation of Microglia in the DRG and DH

To assess CCI-induced mechanical hyperalgesia, we measured the PWT in rats from day 1 to day 21 after CCI. The ipsilateral PWT in CCI rats, compared with that in naive rats, was significantly decreased 1 day after CCI, and this decrease persisted for the entire observation period. These data confirm the development of mechanical hyperalgesia in rats after CCI.

To examine whether nerve injury alters the levels of CSF1 and microglial activity in the ipsilateral DH, we performed immunofluorescence (IF) staining to detect expression of CSF1 and CD11b (a marker of microglia) on day 7 after CCI. CSF1 or CD11b IF in the DH could be observed in both CCI and naive rats, the increase in CD11b was accompanied by an increase in CSF1, and CSF1 acted on the microglia as indicated by colocalization of CSF1 and CD11b IF. Importantly, we found that the CSF1 IF was mostly located in the laminae I-II, a critical region for transmission of pain. Compared with naive rats, CCI rats showed significantly higher fluorescent intensity for both CSF1 and CD11b in the ipsilateral DH at day 7 after CCI.

To further determine the alteration of CSF1 after nerve injury, we measured protein levels of CSF1 in the DRG and the DH on days 1, 3, 7, 14, and 21 after

CCI. The significant increases in protein levels of CSF1 in the DRG were observed on day 1 after CCI and persisted until day 21, with peak increase on day 14. The significant increases in protein levels of CSF1 in the DH were found on day 7 and lasted until day 21, with maximum increases on day 14 (Figure 2).

SCS Produces Analgesia, Attenuates Microglial Activation, and Decreases CSF1 Levels in CCI Rat DH

To assess the analgesia effect of SCS, we delivered SCS and measured the PWT from day 1 to day 5 after SCS. We found that the ipsilateral PWT in the CCI + SCS rats was significantly increased compared with that in CCI + sham SCS rats during SCS. Of note, no difference in the contralateral PWT was found across groups throughout the observation period. We next examined whether SCS alters the CSF1 levels and microglial activation in the ipsilateral DH using IF staining and Western blots in CCI rats after a 5-day SCS treatment. IF study revealed that the fluorescent intensity of both CD11b and CSF1 was markedly increased in the ipsilateral DH of CCI + sham SCS rats as compared to naive rats on day 17 (Figure 3). Of note, CSF1 IF was predominantly distributed in the superficial dorsal horn. Compared with CCI + sham SCS rats, CCI + SCS rats had significantly decreased fluorescent intensity of CD11b and CSF1. Western blot analysis showed that the protein levels of CSF1 in the DH were significantly higher in CCI + sham SCS rats compared with naive rats, but were reduced in CCI + SCS rats.

SCS Attenuates Nerve Injury-Induced Upregulation of Proinflammatory Cytokines in CCI Rat Spinal Cords

Activation of microglia produces proinflammatory cytokines, which are closely associated with the NP. We next examined the effects of SCS on expression of proinflammatory cytokines in the spinal cord in CCI rats after a 5-day SCS treatment (day 17 after CCI). Compared with naive rats, CCI + sham SCS rats exhibited significant increase in mRNA expression of proinflammatory cytokines IL-1 β and TNF- α in the spinal cord, which were both decreased in CCI + SCS rats. No statistical significance in mRNA expression of IL-6 in the spinal cord was found among 3 experimental groups, although mRNA expression of IL-6 in CCI + sham SCS rats trended toward being increased when compared with naive rats (Figure 4).

Intrathecal Injection of Recombinant CSF1 Protein Abolishes Beneficial Effects of SCS on Analgesia and Activation of Microglia in CCI Rat Spinal Cords

To further determine whether the beneficial effects of SCS on analgesia and activation of microglia in the spinal cord are due to downregulation of CSF1, we

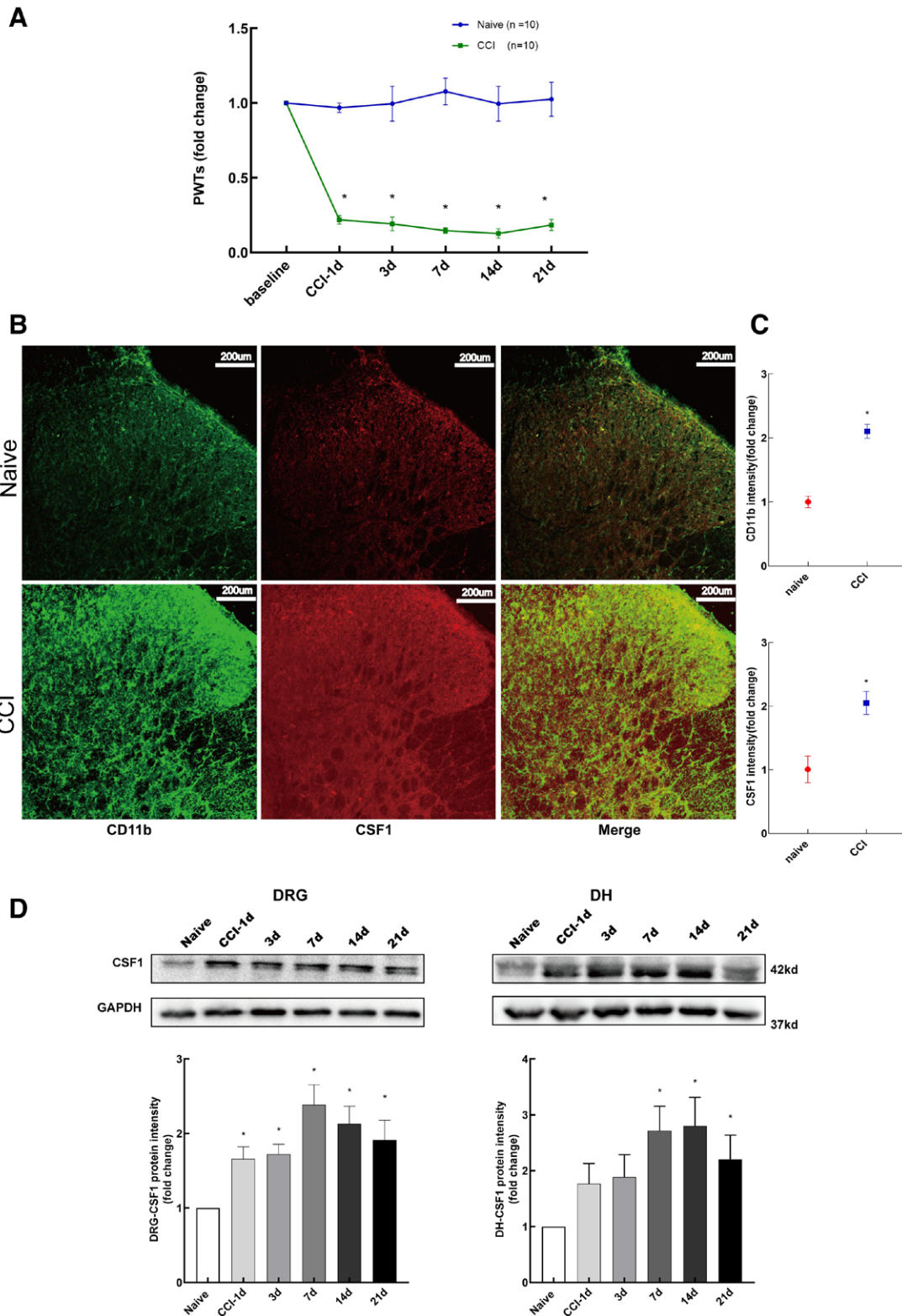


Figure 2. CCI induces hyperalgesia, increases microglial activation in the DH, and augments CSF1 levels in the DRG and DH. A, Time course of a CCI-induced mechanical hyperalgesia as assessed by PWT, ipsilateral to the nerve injury in CCI rats. The naive rats served as control. n = 10 rats/per group; * $P < .0001$, CCI rats versus naive rats. B, Representative immunofluorescence images of CD11b (green) and CSF1 (red) from the ipsilateral DH of CCI rats and naive rats (on day 7 after CCI) (scale bars = 200 μm). C, The intensity of CD11b and CSF1 immunofluorescence in the ipsilateral DH. n = 5 rats/per group; * $P < .0001$ for CD11b and $P = .0003$ for CSF1, CCI rats versus naive rats. D, Western blot analysis of CSF1 in the ipsilateral DRG and the ipsilateral DH at different time points after CCI. For DRG, $P = .036$ for day 1, $P = .00241$ for day 3, $P < .0001$ for day 7, $P = .0004$ for day 14, and $P = .0027$ for day 21. For DH, $P = .6125$ for day 1, $P = .4624$ for day 3, $P = .0215$ for day 7, $P = .0147$ for day 14, and $P = .0269$ for day 21, CCI rats versus naive rats. CCI indicates chronic constriction injury; CD11b, integrin subunit alpha M; CSF1, colony-stimulating factor 1; DH, spinal dorsal horn; DRG, dorsal root ganglion; GAPDH, glyceraldehyde-3-phosphate dehydrogenase; PWTs, paw withdrawal thresholds.

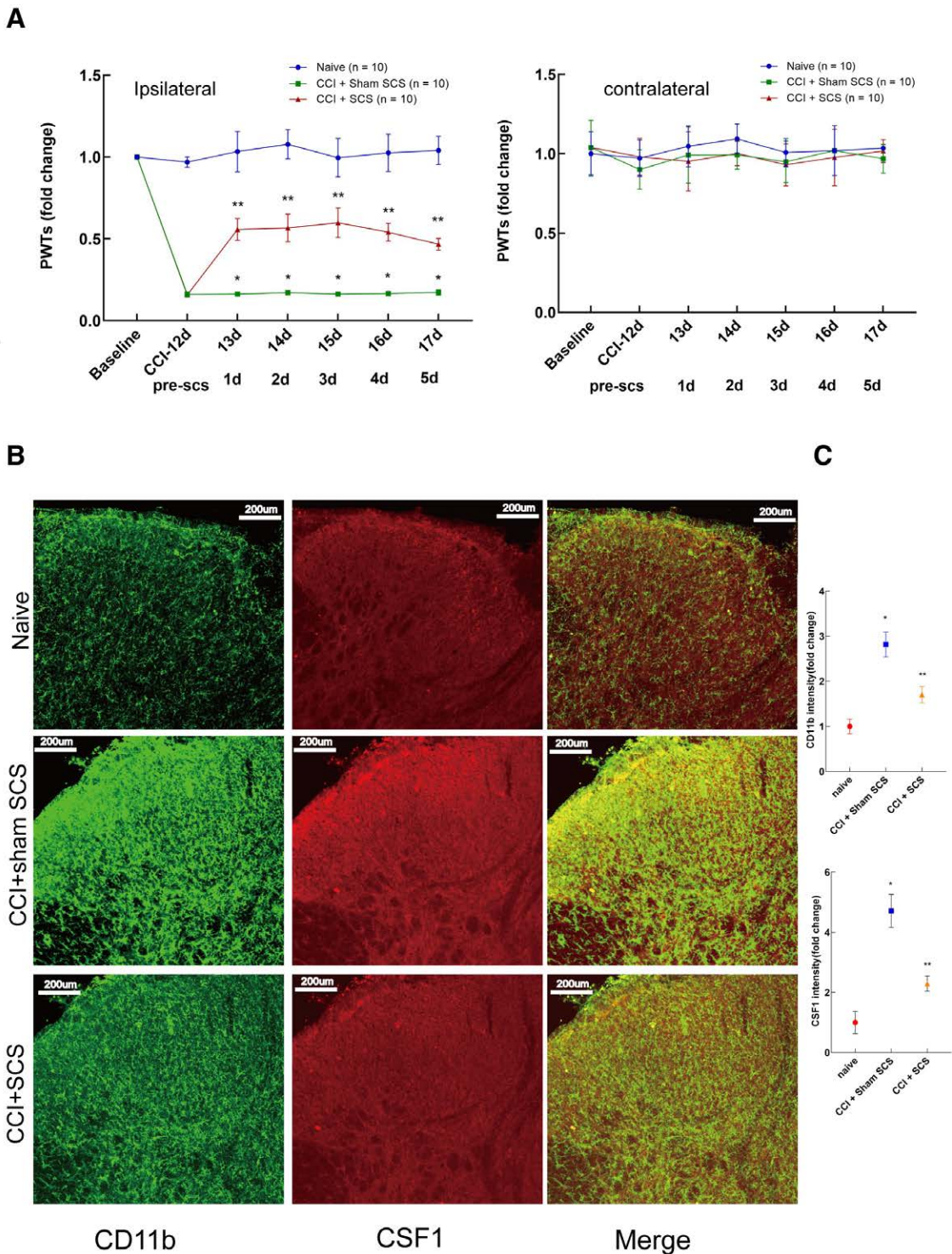


Figure 3. Spinal cord stimulation ameliorates neuropathic pain and reduces immunoreactivity of CD11b and CSF1 in the DH in CCI rats. **A**, Time course of an SCS or a sham SCS–induced change in PWT ipsilateral or contralateral to the nerve injury in CCI rats. The naive rats served as control. $n = 10$ rats/per group; $*P < .0001$, CCI + sham SCS rats versus naive rats; $**P < .0001$, CCI + SCS rats versus CCI + sham SCS rats. **B**, Representative immunofluorescence images of CD11b (green) and CSF1 (red) from the ipsilateral DH on day 17 after CCI (scale bars = 200 μm). **C**, The intensity of CD11b and CSF1 immunofluorescence in the ipsilateral DH. $n = 5$ rats/per group; $*P < .0001$ for CD11b and $P = .0019$ for CSF1, CCI + sham SCS rats versus naive rats; $**P < .0001$ for CD11b and $P = .0343$ for CSF1, CCI + SCS rats versus CCI + sham SCS rats. CCI indicates chronic constriction injury; CD11b, integrin subunit alpha M; CSF1, colony-stimulating factor 1; DH, spinal cord dorsal horn; DRG, dorsal root ganglion; GAPDH, glyceraldehyde-3-phosphate dehydrogenase; PWTs, paw withdrawal thresholds, SCS, spinal cord stimulation.

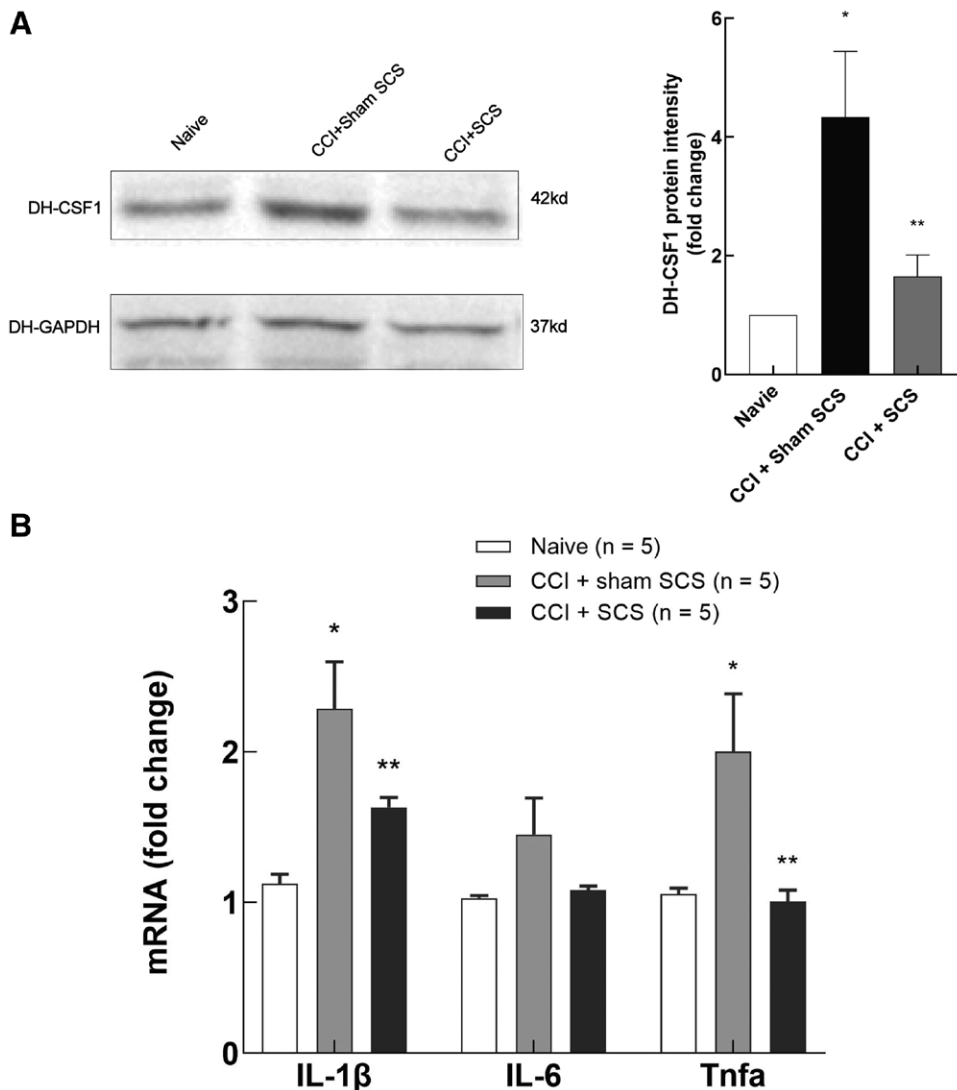


Figure 4. Spinal cord stimulation reduces CSF1 levels and proinflammatory cytokine expression in the DH in CCI rats. A, Western blot analysis of CSF1 levels in the DH; * $P = .0099$, CCI + sham SCS rats versus naive rats; ** $P = .0367$, CCI + SCS rats versus CCI + sham SCS rats. B, Real-time PCR analysis of mRNA expression for proinflammatory cytokines IL-1 β , IL-6, and TNF- α in the DH. $n = 5$ rats/per group; * $P = .0003$ for IL-1 β , $P = .2671$ for IL-6, and $P = .031$ for TNF- α , CCI + sham SCS rats versus naive rats; ** $P = .0494$ for IL-1 β , $P = .3623$ for IL-6, and $P = .0018$ for TNF- α , CCI + SCS rats versus CCI + sham SCS rats. CCI indicates chronic constriction injury; CSF1, colony-stimulating factor 1; DH, spinal dorsal horn; GAPDH, glyceraldehyde-3-phosphate dehydrogenase; IL, interleukin; mRNA, messenger ribonucleic acid; PCR, polymerase chain reaction; SCS, spinal cord stimulation; TNF- α , tumor necrosis factor- α .

performed a once-daily intrathecal injection of recombinant CSF1 protein or trehalose in CCI + SCS rats for 3 days, starting on day 2 after SCS. As expected, daily intrathecal injection of trehalose did not alter the ipsilateral PWT in CCI + SCS rats, whereas daily intrathecal injection of recombinant CSF1 protein reduced the ipsilateral PWT in CCI + SCS rats to the same extent as that observed in CCI + sham SCS rats.

We then performed IF staining on the sections of the L4-L6 spinal cord to examine the effects of intrathecal injection of CSF1 and trehalose on microglial activation in CCI rats. The fluorescent intensity of CD11b in the spinal cord was significantly lower in CCI + SCS + trehalose rats compared with CCI + sham SCS rats (Figure 5) However, the fluorescent intensity

of CD11b in the spinal cord in CCI + SCS + CSF1 rats was markedly higher, similar to that in CCI + sham SCS rats. These data confirm that the effects of SCS on analgesia and activation of microglia in the spinal cord in CCI rats were mediated by downregulation of SCF1.

SCS REDUCES CSF1 LEVELS IN DORSAL ROOTS BUT NOT DRG

We finally investigated the effects of SCS on the levels of CSF1 in the DRG and the dorsal roots in CCI rats after a 5-day SCS treatment (day 17 after CCI). IF study showed that the fluorescent intensity of CSF1 in the DRG and dorsal roots was significantly increased in CCI + sham SCS rats compared with naive rats.

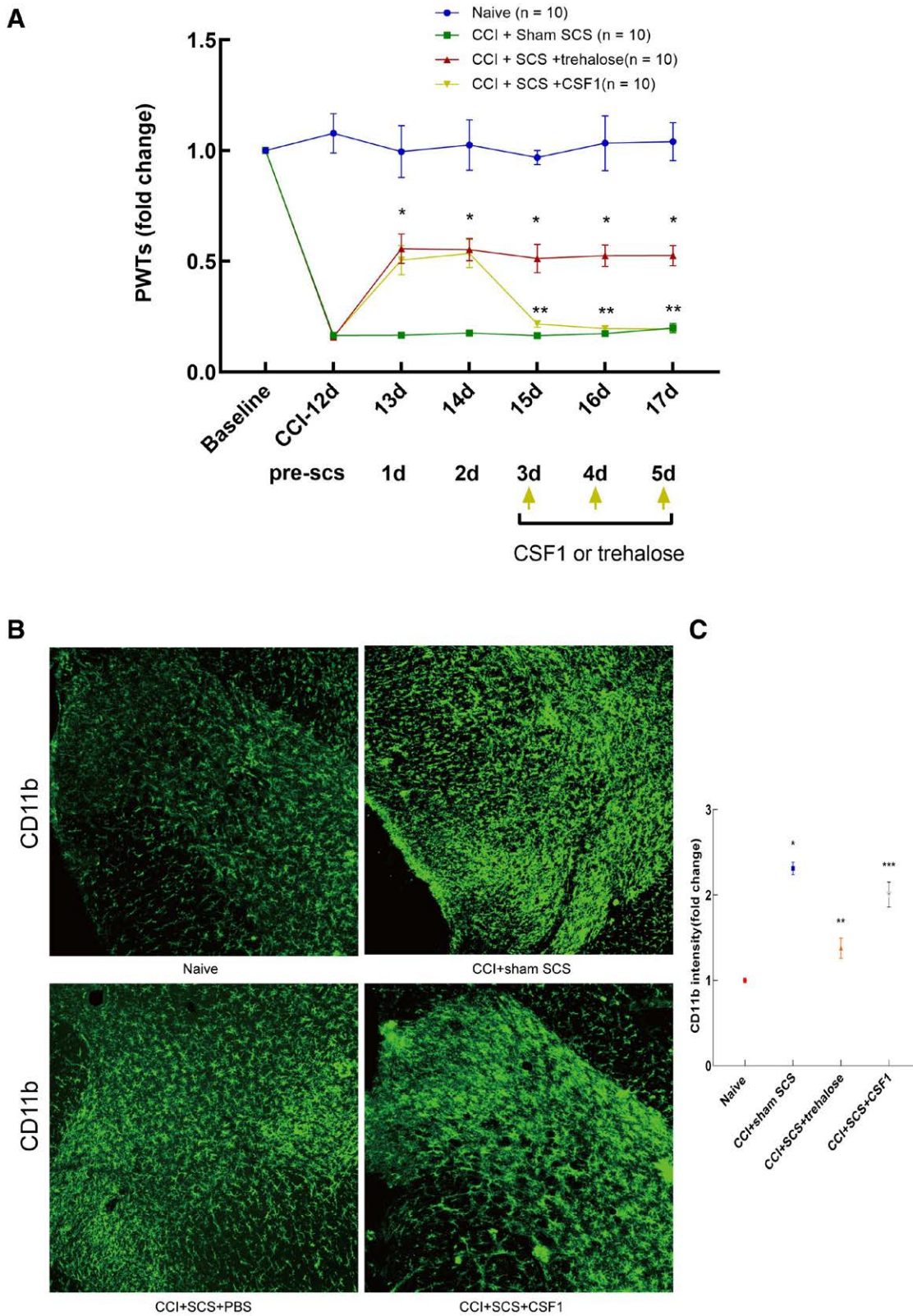


Figure 5. Intrathecal injection of recombinant CSF1 protein abolishes the beneficial effects of SCS on analgesia and activation of microglia in the spinal cord in CCI rats. **A**, Effect of intrathecal injection of recombinant CSF1 or trehalose on PWT ipsilateral to the nerve injury in CCI + SCS rats. The naive rats served as control. n = 10 rats/per group; * $P < .0001$, CCI + SCS + trehalose rats versus CCI + sham SCS rats; ** $P = .0001$, CCI + SCS + CSF1 rats versus CCI + SCS + trehalose rats. **B**, Effect of intrathecal injection of recombinant CSF1 or trehalose on CD11b immunoreactivity in the ipsilateral DH. Scale bars = 200 μm . **C**, The intensity of CD11b immunofluorescence in the ipsilateral DH. n = 5 rats/per group; * $P = .0002$, CCI + sham SCS rats versus naive; ** $P = .0090$, CCI + SCS + trehalose rats versus CCI + sham SCS rats; and *** $P = .0491$, CCI + SCS + CSF1 rats versus CCI + SCS + trehalose rats. CCI indicates chronic constriction injury; CD11b, integrin subunit alpha M; CSF1, colony - stimulating factor 1; DH, spinal dorsal horn; DRG, dorsal root ganglion; PWTs, paw withdrawal thresholds; SCS, spinal cord stimulation.

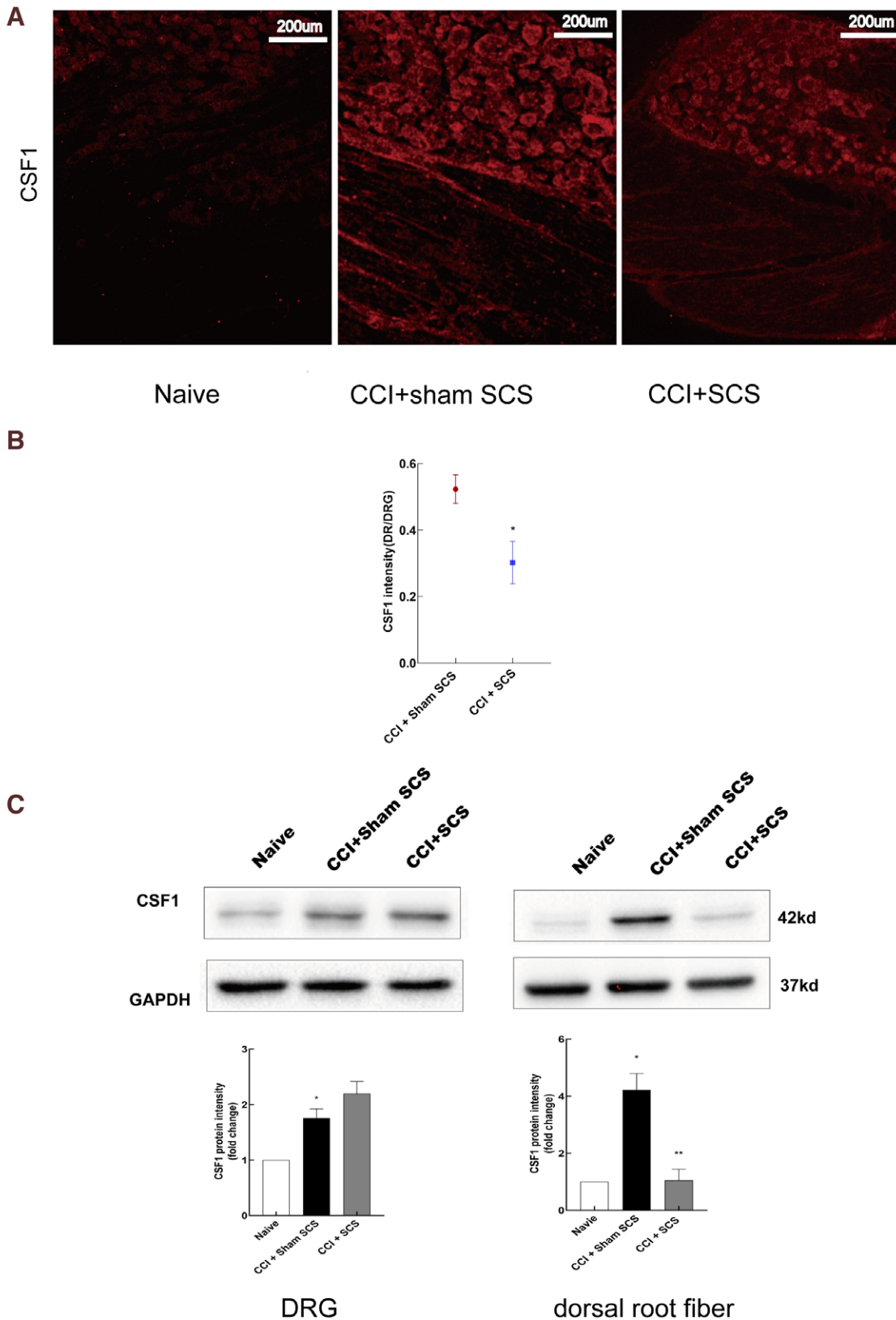


Figure 6. SCS inhibits the release of CSF1 from DRG. A, Effect of SCS on CSF1 immunoreactivity in the ipsilateral DRG and DR (scale bars = 200 μ m). B, The intensity of CSF1 immunofluorescence ratio in DRs to DRG. n = 5 rats/per group; * P = .0089, CCI + SCS rats versus CCI + sham SCS rats. C, Effect of SCS on CSF1 levels in the ipsilateral DRG and DR. n = 5 rats/per group; * P = .0156 for DRG and P < .0001 for DR, CCI + sham SCS rats versus naive rats; ** P < .0001 for DR, CCI + SCS rats versus CCI + sham SCS rats. CCI indicates chronic constriction injury; CSF1, colony-stimulating factor 1; DH, spinal dorsal horn; DR, dorsal root fiber; DRG, dorsal root ganglion; GAPDH, glyceraldehyde-3-phosphate dehydrogenase; SCS, spinal cord stimulation.

However, a 5-day SCS treatment of CCI rats reduced the fluorescent intensity of CSF1 in the dorsal roots but did not alter that in the DRG. Consistent with the IF results, Western blot analysis showed that the protein levels of CSF1 were elevated in both DRG and dorsal roots in CCI + sham SCS rats compared with naive rats. SCS treatment reduced the protein levels of CSF1 in the dorsal roots but not the DRG. These data suggest that SCS might inhibit the transmission of CSF1 from the DRG to the spinal cord (Figure 6).

DISCUSSION

This study reported the novel findings that SCS inhibits the transmission of CSF1 from the DRG to the spinal cord, which reduces microglial activation and proinflammatory cytokine production in the spinal cord, contributing to SCS-induced pain relief in a CCI rat model.

CCI, Hyperalgesia, Microglial Activation, and CSF1

In this study, we chose a CCI rat model, which not only mimics a posttraumatic painful peripheral neuropathy but also maintains the intact C-fibers and A β -fibers.

Our data showed that the decreased PWT occurred from day 1 after CCI and lasted for at least 21 days. The maximum decrease in PWT was observed on day 14 after CCI. These results were consistent with a previous study.²² Western blot analysis showed that the CSF1 levels in the DRG were significantly increased from the first day after nerve injury, while the CSF1 levels in the spinal cord were gradually increased, and the significant increases were found from day 7 after CCI. Moreover, fluorescent intensity of CSF1 in the sections of spinal cords was also significantly higher from day 7 after CCI, which was accompanied by increased fluorescent intensity of microglial marker CD11b and the change of cell morphology, indicating the activated state (from a normal ramified surveillance shape to a reactive hypertrophic shape),⁶ similar to those observed in previous studies.^{6,19} These findings suggest that CSF1, which is produced by the DRG and transported by the dorsal roots into the spinal cord after nerve injury, is an important factor for microglial activation. These findings are in line with the results of a previous study, which showed that CSF1 is produced by damaged DRG and is released to the relative spinal DH via the dorsal roots, where it activates microglia, contributing to the development of NP¹³ (Supplemental Digital Content, Figure 1, <http://links.lww.com/AA/D915>). IF study showed that the CSF1 fluorescence was predominantly located in the superficial layer (LI and LII) of the ipsilateral spinal cord, which indicates the characteristics of nociceptive processing.^{25,26} Taken together, these observations suggest that increased CSF1 expression is produced

in the injured sensory neurons and transported to the spinal cord, where it targets the microglial CSF1 receptor (CSF1R), leading to activation of microglia and subsequent NP.^{13,27} Our findings are supported by a previous study demonstrating that Cre-mediated sensory neuron deletion of CSF1 completely prevents nerve injury-induced mechanical hypersensitivity and reduces microglial activation and proliferation in mice. In contrast, intrathecal injection of CSF1 induces mechanical hypersensitivity and microglial activation not only in mice with sensory neuron deletion of CSF1 but also in wild-type mice.¹³ These results suggest that CSF1 signaling is necessary for the development of NP and is potentially a therapeutic target for treating NP.

SCS Produces Analgesia by Inhibiting Microglial Activation and CSF1 Levels in CCI Model Spinal Cord

Despite that SCS could not normalize the PWT, it caused a significant increase in PWT, indicating that SCS is able to produce analgesic effects in CCI rats. Previous studies reported that a small but significant reduction in mechanical hypersensitivity could persist for up to 5 days in CCI rats even after the cessation of SCS,^{26,28–30} thus, this cannot be completely explained by GCT alone. Our study demonstrated that repeated SCS attenuated microglial activation, as indicated by reduced immunoreactivity of CD11b in the ipsilateral DH in CCI rats, is in agreement with results of previous studies showing that continuous SCS treatment for 4 days relieved NP by inhibiting activation of microglia and astrocytes in the spinal cord of rats with spared nerve injury.^{15,16} Another study showed that SCS reduces chronic cardiac pain partially by inhibiting spinal microglial activation and, thus, potentially downregulates the expression of proinflammatory mediators, such as IL-1 β and TNF- α .³⁰ Moreover, other studies showed that SCS might reduce microglial activation at the level of the spinal cord.^{13,16,20} It is notable that our findings are contrary to results from a recent study showing that conventional SCS exacerbated microglial activation in the lumbar cord of CCI rats during the maintenance phase of NP.¹⁹ In that study, SCS was delivered 3 hours per day for 3 days, which was different from the duration of stimulation (6 hours per day for 5 days) in our study, although the stimulation model was similar between the 2 studies. The duration of stimulation has been suggested to be an important factor influencing the effect of SCS on microglial activation in the spinal DH.¹⁵ Thus, we speculate that the discrepancy might be attributed to the difference in the duration of stimulation.

Interestingly, we found that repeated SCS decreased the immunoreactivity of CSF1 as well as the levels of CSF1 in the spinal cord in CCI rats. Because CSF1 is considered an important factor for activation of microglia,^{13,27} these observations led us to hypothesize

that SCS might attenuate microglial activation by decreasing CSF1 levels in the ipsilateral DH in CCI rats. To confirm our hypothesis, we performed intrathecal injection of a recombinant CSF1 protein into CCI + SCS rats. The results showed that intrathecal injection of CSF1 completely abolished the SCS-induced beneficial effects on analgesia and activation of microglia in CCI rats. These findings confirm our hypothesis that SCS attenuates microglial activation by decreasing CSF1 levels in the spinal cord, contributing to pain relief in CCI rats.

SCS Inhibits CSF1 Release From DRG

We measured the level of CSF1 in the DRG and dorsal roots (spinal side), respectively. Both IF study and Western blot analysis showed that repeated SCS decreased the level of CSF1 in the dorsal roots of CCI rats. Based on these results, we conclude that SCS may affect the release of CSF1 from the ipsilateral nerve-injured DRG but it does not affect the production of CSF1 in the ipsilateral nerve-injured DRG, leading to the reduced CSF1 levels in the spinal cord. To date, no studies have reported how CSF1 is secreted and how nerve injury affects its secretion; however, a few studies have confirmed that after nerve injury, the amount of protein secreted by the distal nerve root increases.³¹ Based on knowledge regarding protein secretion, CSF1 is probably a soluble secretory protein, the secretion of which is affected by the intracellular environment and membrane properties. How SCS reduces CSF1 releases from nerve-injured DRG is unclear. It is well known that the majority of axonal proteins are synthesized in the cell body of neurons and transported along axons. CSF1, which is formed by the cell body of neurons,¹³ might be transported to the axon tip and released into the spinal cord when a nerve impulse arrives at the end of the axon. This process might need Na/K adenosine triphosphate (ATP)ase, which plays a role in the release and transmission of CSF1 from the DRG to the spinal DH. Previous studies have shown that SCS or pulsed radiofrequency reduces the expression of Na/K ATPase in the DRG.^{32,33} We could not exclude the possibility that SCS inhibits CSF1 release from nerve-injured DRG to the spinal DH by down-regulating Na/K ATPase in the DRG. Further studies are needed to address this question.

Study Limitations and Expectations

Although this study provides new insight into the mechanisms by which SCS alleviates chronic NP, our study has some limitations. In addition to the lack of mood assessment tools to assess anxiety and depression,^{34,35} we did not demonstrate how SCS affects CSF1 release from nerve-injured DRG neurons. Moreover, the thermal withdrawal thresholds, which

have been shown to be decreased in CCI models^{36,37} and improved by SCS,³⁷ were not assessed in the present study. A recent study reported that inhibition of microglial activation in the spinal cord increased thermal withdrawal thresholds in the CCI model.³⁶ Further studies are warranted to determine whether SCS-induced reduction in CSF1 in the spinal cord in CCI models contributes to improvement of thermal hypersensitivity as well. ■

DISCLOSURES

Name: Cong Sun, MD.

Contribution: This author helped with experimental design, Western blotting, quantitative real-time reverse transcription polymerase chain reaction, immunofluorescence, and animal model establishment.

Name: Xueshu Tao, MD.

Contribution: This author helped with technical guidance of experimental operations and the establishment of some of the animal model.

Name: Chengfu Wan, MD.

Contribution: This author helped with some of the experimental design.

Name: Xiaojiao Zhang, MS.

Contribution: This author helped establish some of the animal model.

Name: Mengnan Zhao, MD.

Contribution: This author helped with some of the experimental design.

Name: Miao Xu, MS.

Contribution: This author helped establish some of the animal model.

Name: Pinying Wang, MD.

Contribution: This author helped establish some of the animal model.

Name: Yan Liu, MD.

Contribution: This author helped establish some of the animal model.

Name: Chenglong Wang, MD.

Contribution: This author helped establish some of the animal model.

Name: Qi Xi, MD.

Contribution: This author helped establish some of the animal model.

Name: Tao Song, MD, PhD.

Contribution: This author agreed to be accountable for all aspects of the work.

This manuscript was handled by: Jianren Mao, MD, PhD.

REFERENCES

- Melzack R, Wall PD. Pain mechanisms: a new theory. *Science*. 1965;150:971–979.
- Sdrulla AD, Guan Y, Raja SN. Spinal cord stimulation: clinical efficacy and potential mechanisms. *Pain Pract*. 2018;18:1048–1067.
- Barchini J, Tchachaghian S, Shamaa F, et al. Spinal segmental and supraspinal mechanisms underlying the pain-relieving effects of spinal cord stimulation: an experimental study in a rat model of neuropathy. *Neuroscience*. 2012;215:196–208.
- Sherwood CC, Stimpson CD, Raghanti MA, et al. Evolution of increased glia-neuron ratios in the human frontal cortex. *Proc Natl Acad Sci U S A*. 2006;103:13606–13611.
- Ruiz-Sauri A, Orduña-Valls JM, Blasco-Serra A, et al. Glia to neuron ratio in the posterior aspect of the human spinal

- cord at thoracic segments relevant to spinal cord stimulation. *J Anat.* 2019;235:997–1006.
6. Inoue K, Tsuda M. Microglia in neuropathic pain: cellular and molecular mechanisms and therapeutic potential. *Nat Rev Neurosci.* 2018;19:138–152.
 7. Watkins LR, Martin D, Ulrich P, Tracey KJ, Maier SF. Evidence for the involvement of spinal cord glia in subcutaneous formalin induced hyperalgesia in the rat. *Pain.* 1997;71:225–235.
 8. Tawfik VL, Chang SY, Hitti FL, et al. Deep brain stimulation results in local glutamate and adenosine release: investigation into the role of astrocytes. *Neurosurgery.* 2010;67:367–375.
 9. Kim JY, Choi GS, Cho YW, Cho H, Hwang SJ, Ahn SH. Attenuation of spinal cord injury-induced astroglial and microglial activation by repetitive transcranial magnetic stimulation in rats. *J Korean Med Sci.* 2013;28:295–299.
 10. Calvo M, Dawes JM, Bennett DL. The role of the immune system in the generation of neuropathic pain. *Lancet Neurol.* 2012;11:629–642.
 11. Mika J, Rojewska E, Makuch W, Przewlocka B. Minocycline reduces the injury-induced expression of prodynorphin and pronociceptin in the dorsal root ganglion in a rat model of neuropathic pain. *Neuroscience.* 2010;165:1420–1428.
 12. Mika J, Zychowska M, Popiolek-Barczyk K, Rojewska E, Przewlocka B. Importance of glial activation in neuropathic pain. *Eur J Pharmacol.* 2013;716:106–119.
 13. Guan Z, Kuhn JA, Wang X, et al. Injured sensory neuron-derived CSF1 induces microglial proliferation and DAP12-dependent pain. *Nat Neurosci.* 2016;19:94–101.
 14. Johnston IN, Milligan ED, Wieseler-Frank J, et al. A role for proinflammatory cytokines and fractalkine in analgesia, tolerance, and subsequent pain facilitation induced by chronic intrathecal morphine. *J Neurosci.* 2004;24:7353–7365.
 15. Sato KL, Johaneck LM, Sanada LS, Sluka KA. Spinal cord stimulation reduces mechanical hyperalgesia and glial cell activation in animals with neuropathic pain. *Anesth Analg.* 2014;118:464–472.
 16. Shinoda M, Fujita S, Sugawara S, et al. Suppression of superficial microglial activation by spinal cord stimulation attenuates neuropathic pain following sciatic nerve injury in rats. *Int J Mol Sci.* 2020; 21:2390.
 17. Takemoto R, Michihara S, Han LK, Fujita N, Takahashi R. Ninjin'yoeito alleviates neuropathic pain induced by chronic constriction injury in rats. *Front Nutr.* 2021;8:525629.
 18. Muthuraman A, Jaggi AS, Singh N, Singh D. Ameliorative effects of amiloride and pralidoxime in chronic constriction injury and vincristine induced painful neuropathy in rats. *Eur J Pharmacol.* 2008;587:104–111.
 19. Shu B, He SQ, Guan Y. Spinal cord stimulation enhances microglial activation in the spinal cord of nerve-injured rats. *Neurosci Bull.* 2020;36:1441–1453.
 20. Zhao M, Zhang X, Tao X, et al. Sirt2 in the spinal cord regulates chronic neuropathic pain through Nrf2-mediated oxidative stress pathway in rats. *Front Pharmacol.* 2021;12:646477.
 21. Turan Yücel N, Can ÖD, Demir Özkay Ü. Catecholaminergic and opioidergic system mediated effects of reboxetine on diabetic neuropathic pain. *Psychopharmacology (Berl).* 2020;237:1131–1145.
 22. Zhao B, Pan Y, Xu H, Song X. Kindlin-1 regulates astrocyte activation and pain sensitivity in rats with neuropathic pain. *Reg Anesth Pain Med.* 2018;43:547–553.
 23. Agrawal SG, Evans RH. The primary afferent depolarizing action of kainate in the rat. *Br J Pharmacol.* 1986;87:345–355.
 24. Xie JY, Qu C, Munro G, Petersen KA, Porreca F. Antihyperalgesic effects of meteorin in the rat chronic constriction injury model: a replication study. *Pain.* 2019;160:1847–1855.
 25. Colloca L, Ludman T, Bouhassira D, et al. Neuropathic pain. *Nat Rev Dis Primers.* 2017;3:17002.
 26. Cohen SP, Mao J. Neuropathic pain: mechanisms and their clinical implications. *BMJ.* 2014;348:f7656.
 27. Okubo M, Yamanaka H, Kobayashi K, et al. Macrophage-colony stimulating factor derived from injured primary afferent induces proliferation of spinal microglia and neuropathic pain in rats. *PLoS One.* 2016;11:e0153375.
 28. Rees H, Roberts MH. Antinociceptive effects of dorsal column stimulation in the rat: involvement of the anterior pretectal nucleus. *J Physiol.* 1989;417:375–388.
 29. Howard-Quijano K, Yamaguchi T, Gao F, et al. Spinal cord stimulation reduces ventricular arrhythmias by attenuating reactive gliosis and activation of spinal interneurons. *JACC Clin Electrophysiol.* 2021;7:1211–1225.
 30. Wang J, Wu XC, Zhang MM, et al. Spinal cord stimulation reduces cardiac pain through microglial deactivation in rats with chronic myocardial ischemia. *Mol Med Rep.* 2021;24:835.
 31. Zochodne DW. The microenvironment of injured and regenerating peripheral nerves. *Muscle Nerve Suppl.* 2000;9:S33–S38.
 32. Tilley DM, Cedeño DL, Kelley CA, DeMaegd M, Benyamin R, Vallejo R. Changes in dorsal root ganglion gene expression in response to spinal cord stimulation. *Reg Anesth Pain Med.* 2017;42:246–251.
 33. Vallejo R, Tilley DM, Williams J, Labak S, Aliaga L, Benyamin RM. Pulsed radiofrequency modulates pain regulatory gene expression along the nociceptive pathway. *Pain Physician.* 2013;16:E601–E613.
 34. Meyer-Rosberg K, Burckhardt CS, Huizar K, Kvarnström A, Nordfors LO, Kristofferson A. A comparison of the SF-36 and Nottingham Health Profile in patients with chronic neuropathic pain. *Eur J Pain.* 2001;5:391–403.
 35. Twillman RK. Mental disorders in chronic pain patients. *J Pain Palliat Care Pharmacother.* 2007;21:13–19.
 36. Zhang X, Wang J, Sui A, Zhang N, Lv Q, Liu Z. Antinociceptive effect of magnolol in a neuropathic pain model of mouse. *J Pain Res.* 2021;14:2083–2093.
 37. Koyama S, Xia J, Leblanc BW, Gu JW, Saab CY. Subparesthesia spinal cord stimulation reverses thermal hyperalgesia and modulates low frequency EEG in a rat model of neuropathic pain. *Sci Rep.* 2018;8:7181.